Estonian Journal of Earth Sciences, 2014, **63**, 4, 207–213 doi: 10.3176/earth.2014.20

The stratigraphic imprint of a mid-Telychian (Llandovery, Early Silurian) glaciation on far-field shallow-water carbonates, Anticosti Island, Eastern Canada

François Clayer* and André Desrochers

Department of Earth Sciences, University of Ottawa, Ottawa, ON, K1N 6N5, Canada; andre.desrochers@uottawa.ca
* Present address: INRS-ETE, 490 rue de la Couronne, Québec, Qc, G1K 9A9, Canada; Francois.Clayer@ete.inrs.ca

Received 15 July 2014, accepted 3 October 2014

Abstract. The near-field stratigraphic record of the Early Silurian glaciations is well documented in the literature. Data from far-field areas are, however, sparse. One of the best far-field stratigraphic records of these Llandovery glaciations is exposed on Anticosti Island in eastern Canada. Eight shallow-water paleotropical facies are present close to the mid-Telychian Jupiter–Chicotte formational boundary along the south-central coast of Anticosti Island. These can be grouped into three facies associations that include, from bottom to top: a carbonate facies association (FA-1), a mixed siliciclastic and carbonate facies association (FA-2) and an encrinitic facies association (FA-3). These mid- to outer-ramp strata represent deposition mostly from episodic, high-energy storm events as evidenced by their sharp bases, hummocky cross-stratification, large wave ripples, gutter casts and wave-enhanced sediment gravity flow deposits. Superimposed on a long-term regressive trend, one main transgressive–regressive (TR) sequence and four meter-scale TR cycles are evident, indicating a multi-order stratigraphic framework developed under the influence of glacio-eustasy. The Jupiter–Chicotte formational boundary, a regional discontinuity surface caused by a forced regression, corresponds to the onset of a far-field mid-Telychian glaciation.

Key words: far-field record, shallow-water carbonates, mid-Telychian, Anticosti Island.

INTRODUCTION

An Early Silurian glacial record is well established and considered as part of a larger icehouse period, the "Early Palaeozoic Icehouse" (Page et al. 2007). The Llandovery with its proven glacial deposits (Grahn & Caputo 1992; Caputo 1998; Díaz-Martínez & Grahn 2007), and therefore proven glacially induced sea-level fluctuations (Johnson 2006, 2010; Munnecke et al. 2010), should have generated a distinct sedimentological and stratigraphic imprint on far-field paleotropical carbonate platforms. In this study, we used outcrop-based facies analysis, coupled with cycle and sequence stratigraphic analysis, as sedimentary proxies to track the onset of a major mid-Telychian glacial episode in the shallow-water carbonates exposed on Anticosti Island in the Gulf of St Lawrence (Fig. 1).

GEOLOGICAL SETTING

The tectonically undisturbed Anticosti succession was deposited on a rapidly subsiding foreland basin, along the eastern margin of Laurentia in the southern tropical equatorial belt during the Late Ordovician to earliest Silurian (Scotese 2010). The upper 900 m of the >2 km thick Sandbian to Telychian succession constitutes a comprehensive, late Ordovician to early Silurian record superbly exposed on Anticosti Island (Long 2007). Coupled with a sustained sediment supply within a highly subsiding basin, the Anticosti succession is exceptionally thick (e.g. Sandbian to Katian = 1600 m, Hirnantian = ~100 m, Rhuddanian to mid-Telychian = 500 m). This is one or two orders higher than thicknesses of age equivalent carbonate sections deposited in other shallow epeiric or ramp settings (Ghienne et al. 2014).

PREVIOUS WORK

The Jupiter and Chicotte formations are the uppermost units exposed on Anticosti Island (Copper & Long 1990; Brunton & Copper 1994). The east–west trending, ~150 km long outcrop belt of the uppermost Jupiter Formation (Pavillon Member) is slightly oblique to the inferred paleoshoreline, with near-shore mixed siliciclastic–carbonate facies present in the eastern part of Anticosti Island and more offshore carbonate-

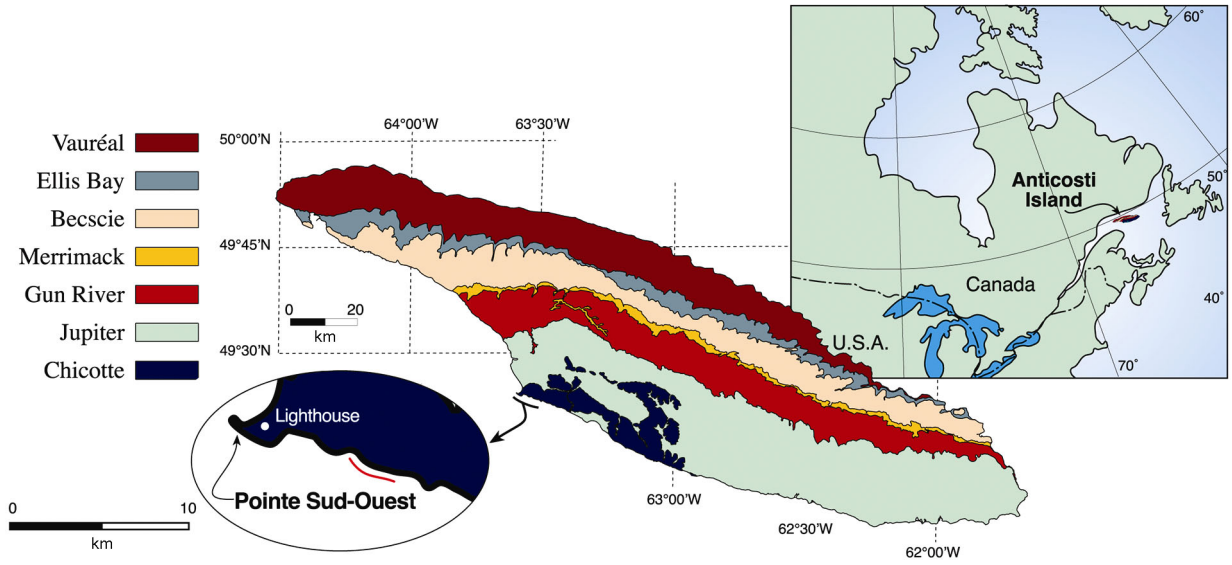

Fig. 1. Location of Anticosti Island and the study area.

dominated facies in the western parts of the island (Clayer 2012). The Chicotte Formation (~90 m thick) is dominated by encrinitic and reefal limestones (Brunton & Copper 1994; Desrochers 2006; Desrochers et al. 2007). The Jupiter–Chicotte formation boundary coincides with the *staurognathoides–eopennatus* conodont zonal boundary indicating a mid-Telychian age (Munnecke & Männik 2009). The Chicotte encrinites represent proximal mid-ramp deposits that prograded over the more distal mid- to outer-ramp facies of the underlying Jupiter Formation in response to long-term sea-level fall during the Telychian (Desrochers 2006).

METHODS

We examined four sections at, or close to the Jupiter–Chicotte formational contact along the south coast of Anticosti Island, but the present study is confined to the coastal section at the Jumpers Cliff (Fig. 2A, B), located east of the Anse Gibbons, about 4 km east of the Southwest Point (UTM 20U 0461091-5469995). The Jumper Cliff section exposes 8 m of the Pavillon Member in the uppermost Jupiter Formation and 6 m of the basal Chicotte Formation (Clayer 2012). Thirty thin sections were made in order to complement field observations.

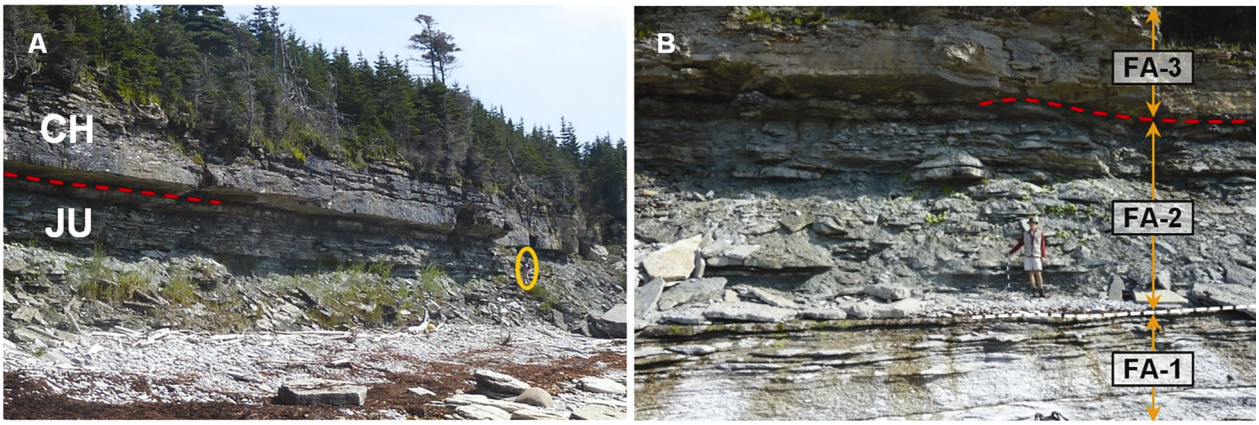

Fig. 2. Exposures of the Jupiter–Chicotte formational boundary exposed along the coastal Jumpers section, in the south-central part of Anticosti Island. Person for scale.

OUTCROP-BASED FACIES ANALYSIS

Eight facies, grouped into three facies assemblages (FA), represent sediments deposited on a mixed siliciclastic–carbonate ramp during the mid-Telychian (see Table 1 for individual facies description and interpretation). Supplementary data on facies are available in Clayer (2012).

Carbonate-dominated FA-1 (Facies 7 and 8) consists of thin, lenticular packstone/grainstone, interbedded with fair-weather bioturbated mudstone/wackestone in the upper Pavillon Member. The lenticular beds, associated with gutter casts and small scoured channels, represent sediments deposited as distal mid- to outer-ramp tempestites under wave-enhanced sediment gravity flows, evolving from combined flows generated higher on the ramp. Large wave ripples are also present.

The assemblage FA-2 includes mixed siliciclastic–carbonate facies (Facies 4–6) in the uppermost Pavillon strata. It comprises bioclastic packstone/grainstone deposited as distal to proximal mid-ramp carbonate tempestites, interbedded with fairweather calcareous

Table 1. Description and interpretation of the facies identified across the Jupiter–Chicotte formational boundary in the Jumpers section

Facies	Composition	Description	Depositional setting
FA-3			
Almagamated encrinites (1)	Pack/grainstone (100%)	***Packstone/grainstone:*** Medium- to thick-bedded (10–50 cm). Massive. Poorly bioturbated. Amalgamated. Sharp base.	Proximal mid-ramp
Coral–stromatoporoid boundstone (2)	Boundstone (≥90%) Calcareous shale (≤10%)	***Boundstone:*** Framework of mainly tabulate corals and stromatoporoids. Matrix of pelloid-rich wackestone/packstone. Shale interbeds of interbioherm cut through. Interbioherm facies consists of Facies 3.	Proximal mid-ramp
Encrinites interbedded with calcareous shale (3)	Pack/grainstone (90%) Calcareous shale (10%)	***Packstone/grainstone:*** Thin- to thick-bedded (5–50 cm). Massive. Moderately bioturbated. Mostly amalgamated but also with calcareous shale interbeds. ***Calcareous shale:*** Very thin (0–3 cm). Fissile.	Mid-ramp
FA-2			
Bioclastic pack/grainstone with calcareous shale interbeds (4)	Pack/grainstone (40–70%) Rudstone (≈10%) Calcareous shale (20–50%)	***Packstone/grainstone:*** Thin- to thick-bedded (5–40 cm). Lenticular to subtabular. Discontinuous and sharp-based. Locally bioturbated at top. Sharp base. ***Calcareous shale:*** Very thin to thin-bedded (1–10 cm). Fissile to subnodular.	Distal mid-ramp
Nodular bioclastic pack/grainstone interbedded with calcareous shale (5)	Pack/grainstone (40–70%) Calcareous shale (30–60%)	***Packstone/grainstone:*** Thin- to medium-bedded (5–15 cm). Nodular to subtabular. Discontinuous. Locally bioturbated. ***Calcareous shale:*** Very thin to thin-bedded (2–5 cm). Fissile.	Distal mid-ramp
Calcareous shale (6)	Calcareous shale (100%)	***Calcareous shale:*** Very thin to thick-bedded (1–30 cm). Fissile to subnodular.	Outer ramp to distal mid-ramp
FA-1			
Bioclastic pack/grainstone with bioturbated mud/wackestone interbeds (7)	Pack/grainstone (30–60%) Mud/wackestone (40–70%)	***Packstone/grainstone:*** Thin- to thick-bedded (5–40 cm). Lenticular. Discontinuous. Sharp-based, commonly graded and locally laminated on top. Locally bioturbated. ***Mudstone/wackestone:*** See below (9).	Distal mid-ramp
Bioturbated mud/wackestone (8)	Mud/wackestone (100%)	***Mudstone/wackestone:*** Thin-bedded (5–10 cm). Tabular to subnodular. Continuous. Intensively bioturbated.	Outer ramp to distal mid-ramp

shale (Facies 6). Hummocky cross-stratification, sharp basal contacts, gutter casts and graded beds suggest sedimentation from erosive combined to waning flows (Dumas et al. 2005; Dumas & Arnott 2006). Large wave ripples with low-angle cross-stratification were generated by combined flows, but in the more distal mid-ramp setting, where the relatively weak unidirectional current allowed the bedforms to migrate preferentially (Dumas & Arnott 2006). Abundant calcareous shale interbeds suggest the presence of persistent mud plumes transported by geostrophic and longshore currents, and derived from a delta located at a distance at the basin margin (Clayer 2012). The diverse brachiopod fauna associated with FA-2 supports our paleobathymetric interpretation (Copper & Long 1990).

Encrinitic FA-3 (Facies 1–3) in the basal Chicotte strata includes graded beds with sharp basal contacts, indicating sediment reworking and rapid deposition from episodic, high-energy storm events. Coarse-grained amalgamated encrinites (Facies 1) represent sediments that were deposited in a more proximal mid-ramp settings than Facies 3. Fair-weather and/or deeper-water fine-grained deposits (Facies 6) are only locally present, as this material either did not have time to accumulate between storm events, or was reworked by erosion prior to the deposition of the next encrinitic bed. Local coral-stromatoporoid boundstone (Facies 2) forms distinct sub-meter thick bioherms laterally passing into thinner bio-stromal units (described in Brunton 1988). The bioherm faunal assemblage indicates maximum water depths of 20–30 m (Brunton & Copper 1994) consistent with our interpretation.

CYCLE AND SEQUENCE STRATIGRAPHY

The section can be divided, in terms of a sequence stratigraphic nomenclature, into major transgressive–regressive (TR) sequences and minor meter-scale TR cycles (Embry et al. 2007). Each sequence is confined by an upper and a lower sequence boundary (SB) that can be either conformable or unconformable. Each TR sequence or cycle shows a lower deepening transgressive and upper shallowing regressive unit, separated by a maximum flooding zone. Three orders of stratigraphic units are present in the measured section, which displays part of an overall shallowing trend, formed during Telychian time, on which a complete TR sequence and four meter-scale TR cycles are superimposed (Fig. 3).

The long-term regressive trend is partially captured by the transition from distal mid- to outer-ramp isolated tempestites (FA-1 and FA-2) to proximal mid-ramp amalgamated encrinites (FA-3). The complete TR sequence includes 5 m of the uppermost Jupiter Formation (FA-2) and 4 m of the basal Chicotte Formation (FA-3). Its lower SB is placed at the top of the first shallowing-upward package (3 m above the base of the section in Fig. 3: top of FA-1) and corresponds to a maximum regressive surface (MRS). The lower transgressive system track (TST) forms only the first meter of the section where shale interbeds are abundant. The upper thicker regressive system track (RST) ends at the top of the first coarse-grained encrinitic package in the basal Chicotte Formation (8.2 m level). This RST is characterized by an abrupt shift in depositional environment from distal mid-ramp tempestites (Facies 4 + 5) to proximal mid-ramp amalgamated encrinites (Facies 1) at the Jupiter–Chicotte formational boundary (Fig. 2A, B). This sharp contact represents a forced regressive surface of marine erosion, the first of several regressive surfaces identified higher in the Chicotte Formation (Desrochers 2006). The upper SB is a composite MRS recording a phase of subaerial exposure modified later by physical coastal erosion during the ensuing transgression. This MRS is overlain by recessive calcareous shale associated with a rapid flooding event.

The four meter-scale TR cycles are recording complex, but repetitive sea-level fluctuations superimposed on the larger TR sequence and are clearly reflected in the coastal cliff weathering profile (Fig. 3). The upper Jupiter strata (FA-2) display two meter-scale TR cycles. In the lower Chicotte Formation (FA-3), two TR cycles are present, showing alternating changes between bio-turbated fine-grained muddy encrinites (Facies 3) and thicker-bedded and coarser clean encrinites (Facies 1). Small coral–stromatoporoid bioherms are locally present within the lower meter-scale Chicotte TRS, but were unable to keep up with relative sea-level rise and thus gave up.

In summary, the Jupiter–Chicotte formational boundary represents a disconformable stratigraphic surface with a significant depositional facies offset due to a forced regression.

DISCUSSION

Based on our facies analysis, the Anticosti depositional ramp was under a sedimentary regime dominated by storms, not only during the deposition of the Jupiter and Chicotte formations, but also during the entire Llandovery (Sami & Desrochers 1992; Long 2007). The rate of accommodation space was controlled by tectonic subsidence and sea-level changes (Long 2007).

Anticosti Island, as part of the Appalachian foreland basin, underwent tectonic subsidence under the influence of Taconian and Early Acadian Orogenies (Bordet et al. 2010). The progression of the Taconian deformation

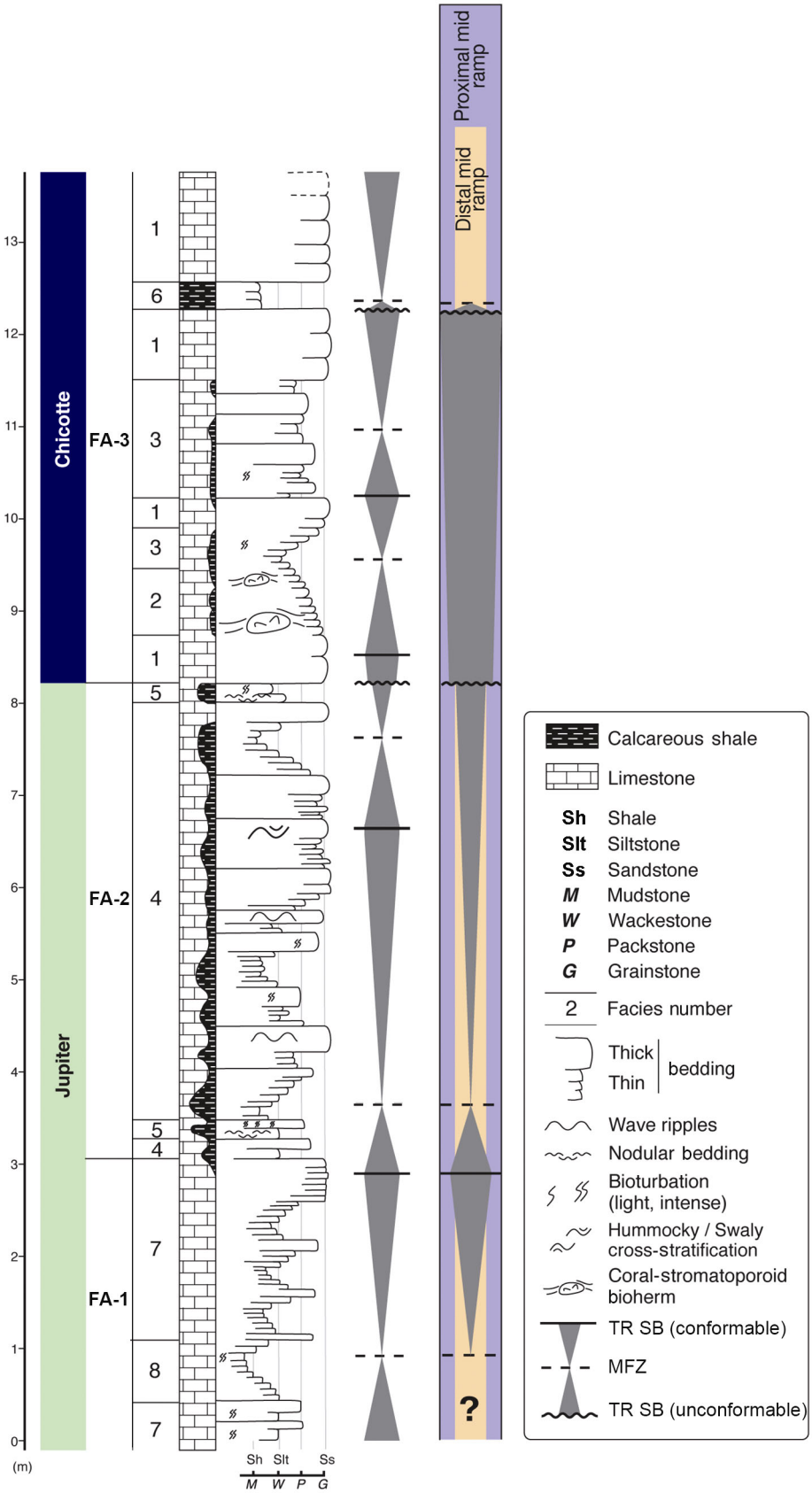

Fig. 3. Detailed stratigraphic log of the Jumpers section with facies, cycles and sequence distribution (see text for details).

front, south of Anticosti, provided sufficient tectonic load to allow the whole Anticosti Platform to subside. According to Long (2007), tectonic, plus sediment-load induced subsidence rates peaked (up to 17.87 cm/ka^{-1}) during the Late Ordovician and declined rapidly (to 1–3 cm/ka^{-1}) beginning in the Hirnantian and falling to ~0.2 cm/ka^{-1} during the Telychian. The overall shallowing trend present in the upper Jupiter and Chicotte formations is driven by a long-term sea-level fall linked to either the decreasing rate of tectonic subsidence and/or a longer-term eustatic signal.

Relative sea-level changes are well defined in our sections, as illustrated by lithological, sedimentological and stratigraphic features (Fig. 3). We observed complex, but repetitive facies transitions corresponding to important temporal shifts of depositional facies belts onto the Anticosti ramp. Our 13 m thick Early Telychian section represents a time interval of about 0.5 Ma (Long 2007; Munnecke & Männik 2009). The only process known to generate such high-frequency sea-level cyclic changes with significant amplitude in the order of several tens of meters is glacio-eustacy. Our main TR sequence and its four smaller-scale TR cycles are likely tuned on the long- (400 Ka) and short- (100 Ka) term eccentricity orbital periodicities, respectively. A scenario that is similar to more recent and well-documented late Cenozoic glaciations.

Evidences for a glacial episode during the Llandovery are undisputable (Grahn & Caputo 1992; Díaz-Martínez & Grahn 2007; Loydell 2007; Munnecke et al. 2010; Ghienne et al. 2013). A Telychian glacial episode is well known from South American glacial deposits (Grahn & Caputo 1992; Caputo 1998). Lowering of atmospheric CO_2 in the late Aeronian–early Telychian triggered a global decrease in temperature and the start of polar ice sheet development (Gouldey et al. 2010). Although debatable (Munnecke et al. 2010), geochemical evidence also suggests a third glacial maximum of the Early Paleozoic Icehouse during the late Telychian (Page et al. 2007). The embedded multi-order stratigraphic architecture and forced regressive surface at the Jupiter–Chicotte formational boundary constitute the far-field imprint associated with orbitally controlled climatic oscillations that lead to recurring ice-sheet growth stages. Similar stratigraphic imprints have been reported for other parts of the Anticosti succession (Desrochers 2006; Long 2007; Desrochers et al. 2010).

CONCLUSIONS

Eight facies, grouped into three facies associations (FA-1 to FA-3), are present near the Jupiter–Chicotte formational boundary along the south coast of Anticosti Island. These facies represent sediment deposited on a storm-dominated mid- to outer carbonate ramp. Their stratigraphic architecture indicates a single TR sequence upon which four smaller meter-scale TR cycles are superimposed. This multi-order stratigraphic motif records high-frequency glacio-eustatic fluctuations forced by a distinct mid-Telychian glacial episode. The main TR sequence is probably driven by the long-term eccentricity orbital forcing (~400 Ka), whereas the smaller meter-scale cycles are of shorter duration (~100 Ka). The Jupiter–Chicotte formational boundary represents a distinct discontinuity surface linked to a forced regression, providing additional evidence of rapid far-field glacial expansion during the mid-Telychian.

Acknowledgments. This work is part of Clayer's M.Sc. thesis at the University of Ottawa. We gratefully acknowledge the residents of Anticosti Island for their help and support during fieldwork. Reviews by D. G. F. Long and K. Histon contributed to an improvement of the manuscript. We also thank Pierre Bertrand for drafting our figures. This work was supported by an internal grant of the University of Ottawa to A. D. This is a contribution to the International Geoscience Programme (IGCP) Project 591 'The Early to Middle Palaeozoic Revolution'.

REFERENCES

Bordet, E., Malo, M. & Kirkwood, D. 2010. A structural study of Western Anticosti Island, St. Lawrence Platform, Québec: a fracture analysis that integrates surface and subsurface structural data. *Bulletin of Canadian Petroleum Geology*, **58**, 36–55.

Brunton, F. R. 1988. *Silurian (Llandovery–Wenlock) Patch Reef Complexes of the Chicotte Formation, Anticosti Island, Québec*. M.Sc. thesis, Laurentian University, Sudbury, Ontario, Canada, 190 pp.

Brunton, F. R. & Copper, P. 1994. Paleoecologic, temporal, and spatial analysis of Early Silurian reefs of the Chicotte Formation, Anticosti Island, Québec, Canada. *Facies*, **31**, 57–80.

Caputo, M. V. 1998. Ordovician–Silurian glaciations and global sea-level changes. In *Silurian Cycles: Linkages of Dynamic Stratigraphy with Atmospheric, Oceanic, and Tectonic Changes* (Landing, E. & Johnson, M. E., eds), *New York State Museum Bulletin*, **491**, 15–25.

Clayer, F. 2012. *Sediment Dynamics and Stratigraphic Architecture of a Lower Silurian Storm-Dominated Carbonate Ramp, Anticosti Island, Québec, Canada*. M.Sc. thesis, University of Ottawa, Ottawa, Québec, Canada, 85 pp., www.ruor.uottawa.ca/bitstream/10393/23149/1/Clayer_Francois_2012-thesis.pdf [accessed 2 October 2014].

Copper, P. & Long, D. G. F. 1990. Stratigraphic revision of the Jupiter Formation, Anticosti Island, Canada; a major reference section above the Ordovician–Silurian Boundary. *Newsletters on Stratigraphy*, **23**, 11–36.

Desrochers, A. 2006. Rocky shoreline deposits in the Lower Silurian (Upper Llandovery, Telychian) Chicotte Formation, Anticosti Island, Québec. *Canadian Journal of Earth Sciences*, **43**, 1205–1214.

Desrochers, A., Bourque, P.-A. & Neuweiler, F. 2007. Diagenetic versus biotic accretionary mechanisms of bryozoan-sponge buildups (Lower Silurian, Anticosti Island, Canada). *Journal of Sedimentary Research*, **77**, 564–571.

Desrochers, A., Farley, C., Achab, A., Asselin, E. & Riva, J. F. 2010. A far-field record of the End Ordovician Glaciation: the Ellis Bay Formation, Anticosti Island, Eastern Canada. *Palaeogeography, Palaeoclimatology, Palaeoecology*, **296**, 248–263.

Díaz-Martínez, E. & Grahn, Y. 2007. Early Silurian glaciation along the western margin of Gondwana (Peru, Bolivia and northern Argentina): palaeogeographic and geodynamic setting. *Palaeogeography, Palaeoclimatology, Palaeoecology*, **245**, 62–81.

Dumas, S., Arnott, R. W. C. & Southard, J. B. 2005. Experiments on oscillatory-flow and combined flow bed forms: implications for interpreting parts of the shallow marine rock record. *Journal of Sedimentary Research*, **75**, 501–513.

Dumas, S. & Arnott, R. W. C. 2006. Origin of hummocky and swaley cross-stratification – the controlling influence of unidirectional current strength and aggradation rate. *Geology*, **34**, 1073–1076.

Embry, A., Johannessen, E., Owen, D., Beauchamp, B. & Gianolla, P. 2007. Sequence Stratigraphy as a "concrete" stratigraphic discipline. In *Report of the ISSC Task Group on Sequence Stratigraphy*, 1–104.

Ghienne, J.-F., Moreau, J., Degermann, L. & Rubino, J.-L. 2013. Lower Palaeozoic unconformities in an intracratonic platform setting: glacial erosion versus tectonics in the eastern Murzuq Basin (southern Libya). *International Journal of Earth Sciences*, **102**, 455–482.

Ghienne, J.-F., Desrochers, A., Paris, F., Achab, A., Asselin, E., Loi, A., Dabard, M.-P., Farley, C., Wickson, S. & Veizer, J. 2014. A Cenozoic-style scenario for the end-Ordovician glaciation. *Nature Geoscience*, doi: 10.1038/ncomms5.

Gouldey, J. C., Saltzman, M. R., Young, S. A. & Kaljo, D. 2010. Strontium and carbon isotope stratigraphy of the Llandovery (Early Silurian): implications for tectonics and weathering. *Palaeogeography, Palaeoclimatology, Palaeoecology*, **296**, 264–275.

Grahn, Y. & Caputo, M. V. 1992. Early Silurian glaciations in Brazil. *Palaeogeography, Palaeoclimatology, Palaeoecology*, **99**, 9–15.

Johnson, M. E. 2006. Relationship of Silurian sea-level fluctuations to oceanic episodes and events. *GFF*, **128**, 115–121.

Johnson, M. E. 2010. Tracking Silurian eustasy: alignment of empirical evidence or pursuit of deductive reasoning? *Palaeogeography, Palaeoclimatology, Palaeoecology*, **296**, 276–284.

Long, D. G. F. 2007. Tempestite frequency curves: a key to Late Ordovician and Early Silurian subsidence, sea-level change, and orbital forcing in the Anticosti Foreland Basin, Québec, Canada. *Canadian Journal of Earth Sciences*, **44**, 413–431.

Loydell, D. K. 2007. Early Silurian positive $\delta^{13}C$ excursions and their relationship to glaciations, sea-level changes and extinction events. *Geological Journal*, **42**, 531–546.

Munnecke, A. & Männik, P. 2009. New biostratigraphic and chemostratigraphic data from the Chicotte Formation (Llandovery, Anticosti Island, Laurentia) compared with the Viki core (Estonia, Baltica). *Estonian Journal of Earth Sciences*, **58**, 159–169.

Munnecke, A., Calner, M., Harper, D. A. T. & Servais, T. 2010. Ordovician and Silurian sea-water chemistry, sea level, and climate: a synopsis. *Palaeogeography, Palaeoclimatology, Palaeoecology*, **296**, 389–413.

Page, A., Zalasiewicz, J., Williams, M. & Popov, L. 2007. Were transgressive black shales a negative feedback modulating glacioeustasy in the Early Palaeozoic Icehouse? In *Deep-Time Perspectives on Climate Change: Marrying the Signal from Computer Models and Biological Proxies* (Williams, M., Haywood, A. M., Gregory, F. J. & Schmidt, D. N., eds), pp. 123–156. Special Publication of the Geological Society of London, The Micropalaeontological Society.

Sami, T. & Desrochers, A. 1992. Episodic sedimentation on an Early Silurian storm-dominated carbonate ramp, Becscie and Merrimack Formations, Anticosti Island, Canada. *Sedimentology*, **39**, 355–381.

Scotese, C. R. 2010. PALEOMAP website. http://www.scotese.com [accessed 2 October 2014].